Journal of Power Sources 195 (2010) 4704–4708

Contents lists available at ScienceDirect

Journal of Power Sources

journal homepage: www.elsevier.com/locate/jpowsour

Short communication

$La_{0.6}Sr_{0.4}Co_{0.2}Fe_{0.8}O_{3-\delta}$ cathodes infiltrated with samarium-doped cerium oxide for solid oxide fuel cells

Lifang Nie [a,b], Mingfei Liu [a], Yujun Zhang [b], Meilin Liu [a,*]

[a] School of Materials Science and Engineering, Georgia Institute of Technology, Atlanta, GA 30332-0245, USA
[b] Key Laboratory for Liquid-Solid Structural Evolution and Processing of Materials (Ministry of Education), Shandong University, Jinan 250061, China

ARTICLE INFO

Article history:
Received 14 January 2010
Received in revised form 17 February 2010
Accepted 17 February 2010
Available online 25 February 2010

Keywords:
LSCF
Cathode
SDC
Infiltration method
SOFC

ABSTRACT

Porous $La_{0.6}Sr_{0.4}Co_{0.2}Fe_{0.8}O_{3-\delta}$ (LSCF) cathodes are coated with a thin film of $Sm_{0.2}Ce_{0.8}O_{1.95-\delta}$ (SDC) using a one-step infiltration process. Examination of the microstructures reveals that small SDC particles are formed on the surface of LSCF grains with a relatively narrow size distribution. Impedance analysis indicates that the SDC infiltration has dramatically reduced the polarization of LSCF cathode, reaching interfacial resistances of 0.074 and 0.44 $\Omega\,cm^2$ at 750 °C and 650 °C, respectively, which are about half of those for LSCF cathode without infiltration of SDC. The activation energies of the SDC infiltrated LSCF cathodes are in the range of 1.42–1.55 eV, slightly lower than those for a blank LSCF cathode. The SDC infiltrated LSCF cathodes have also shown improved stability under typical SOFC operating conditions, suggesting that SDC infiltration improves not only power output but also performance stability and operational life.

© 2010 Elsevier B.V. All rights reserved.

1. Introduction

Solid oxide fuel cells (SOFCs) are attractive energy-conversion devices due to their high energy efficiency, low pollutant emissions and excellent fuel flexibility [1]. Significant efforts are, however, still necessary to develop new generation of SOFCs, that are cost effective and have long operational life. One widely accepted approach is to reduce the operating temperature of SOFCs in order to widen the selectivity of component materials and improve the reliability of SOFC system. Unfortunately, the SOFC power output decreases exponentially as the operating temperature is reduced [2,3].

Since the resistive contribution of the electrolyte can be reduced by decreasing the thickness of electrolyte using electrode-supported cell structures [4,5], The overall performance loss is dominated primarily by the polarization loss of the electrode reactions, especially from the cathode [6]. To enhance the cathode performance at reduced temperatures (La, Sr)(Co, Fe)$O_{3-\delta}$ perovskite oxides have been widely used as cathode materials for SOFCs because of their high electronic and ionic conductivities in the temperature range of 600–800 °C. While cells with (La, Sr)(Co, Fe)$O_{3-\delta}$ cathodes offer significantly higher power densities than those with La(Sr)MnO_3 cathodes, long-term stability of LSCF cathodes seems to be a concern [7].

The electrocatalytic activity of cathode can be improved by adding oxygen ion conducting phases such as doped ceria to LSCF. Dusastre and Kilner [8] studied composite cathodes consisting of LSCF and $Ce_{0.9}Gd_{0.1}O_{2-\delta}$ (GDC) on a GDC electrolyte, achieving an electrode polarization resistance of 0.6 $\Omega\,cm^2$ at 590 °C (with 36 vol% GDC addition), in contrast to 4 $\Omega\,cm^2$ for pure LSCF cathode under the same testing conditions. It was later reported that the polarization resistance of LSCF/$Ce_{0.8}Sm_{0.2}O_{2-\delta}$ (SDC) composite cathodes on YSZ electrolyte was 0.548 $\Omega\,cm^2$ at 700 °C and 0.28 $\Omega\,cm^2$ at 750 °C [9]. Recently, infiltration (or impregnation) processes have been used to fabricate composite electrodes by introducing a thin film of the catalyst onto a porous supporting structure. Jiang et al. [10] developed a novel GDC–LSM composite cathode using multiple-step impregnations process, achieving electrode polarization resistance of ~0.22 $\Omega\,cm^2$ as compared to 26.4 $\Omega\,cm^2$ for pure LSM electrodes at 700 °C. Shah and Barnett [11] studied the infiltration of $La_{0.6}Sr_{0.4}Co_{0.2}Fe_{0.8}O_{3-\delta}$ into porous GDC scaffolds, achieving a polarization resistance of 0.24 $\Omega\,cm^2$ at 600 °C (after firing at 800 °C) and demonstrating that the cathode was stable at 650 °C for over 300 h. Recently, J. Chen et al. [12] reported that the infiltration of palladium and GDC into $La_{0.8}Sr_{0.2}Co_{0.5}Fe_{0.5}O_{3-\delta}$ cathodes had reduced the cathode polarization resistance.

In this paper, we report the findings of our study on SDC infiltrated LSCF cathodes. The porous LSCF backbone was infiltrated with SDC solutions using a one-step infiltration process. The performance and stability of LSCF cathode can be significantly enhanced by a SDC coating.

* Corresponding author. Tel.: +1 404 894 6114; fax: +1 404 894 9140.
E-mail address: meilin.liu@mse.gatech.edu (M. Liu).

0378-7753/$ – see front matter © 2010 Elsevier B.V. All rights reserved.
doi:10.1016/j.jpowsour.2010.02.049

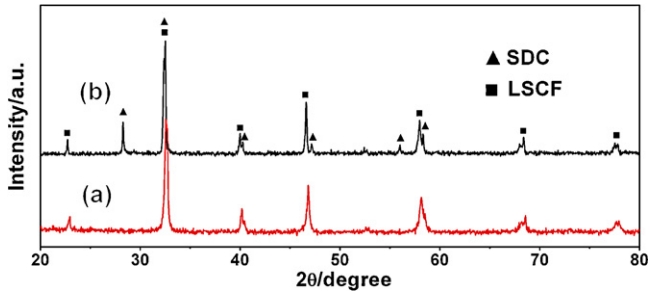

Fig. 1. XRD patterns of (a) blank LSCF (from Fuelcell Material Co.) cathode fired at 1080 °C for 2 h and (b) SDC infiltrated LSCF cathode after fired at 900 °C for 1 h.

2. Experimental

The YSZ electrolyte membranes were fabricated from 8 mol% Y_2O_3-doped ZrO_2 (TZ-8Y, Tosoh, Japan) using tapecasting and sintering at 1450 °C for 5 h. $La_{0.6}Sr_{0.4}Co_{0.2}Fe_{0.8}O_{3-\delta}$ powders with surface area of 5.4 $m^2\,g^{-1}$ were purchased from Fuelcell Material Co., US. The LSCF cathode film was fabricated by tapecasting and then cut into disks with area of 0.3 cm^2. To avoid the reaction between LSCF cathode and YSZ electrolyte, a $Sm_{0.2}Ce_{0.8}O_{1.95}$ (SDC) buffer layer was applied by drop coating SDC slurry on both sides of YSZ pellets. Then LSCF green tapes were bonded to the buffer layer to form LSCF|SDC|YSZ|SDC|LSCF symmetric cells. After dried at 80 °C for 1 h and fired at 1080 °C for 2 h, porous LSCF electrodes (~60 μm thick) were obtained.

Aqueous nitrate solutions of $Sm_{0.2}Ce_{0.8}O_{1.95}$ precursors with different concentrations (0.05, 0.10, 0.25, 0.35 mol L^{-1}) were prepared by dissolving proper amount of $Sm(NO_3)_3{\cdot}6H_2O$ and $Ce(NO_3)_3{\cdot}6H_2O$ in water. Glycine was also added to the solution as a complex agent to form the desired perovskite phase. Propanol was added into the aqueous solution with a ratio of 0.6:1 to improve the wetting on the LSCF backbone. 10 μL of solution was then infiltrated into each side of porous LSCF electrode using a microliter syringe to control the amount of SDC loading. The infiltrated cell was fired at 900 °C for 1 h to obtain the desired SDC phase.

Two Pt meshes were then attached to the LSCF cathodes as current collector for electrochemical measurements. Impedance spectra of the cells at open circuit voltage were acquired using a Solartron impedance analyzer (Solartron 1255 and 1286) in air at temperatures from 650 to 800 °C. The amplitude of the AC signal was 10 mV in a frequency range from 0.01 Hz to 100 kHz. All data were collected after the desired test temperature was reached at least 30 min. Data was corrected for electrode area (0.30 cm^2), and divided by two (symmetric cell) to obtain the actual interfacial polarization resistance of each electrolyte/electrode interface. Button cells with and without the infiltration of SDC were measured with humidified hydrogen (3 vol% H_2O) as fuel and stationary air as oxidant to evaluate the stability of cathode performance.

An X'Pert PRO Alpha-1 X-ray diffractometer (with Cu Kα radiation) was used for phase identification and a LEO 1530 thermally assisted field emission scanning electron microscope was used for microstructure examination.

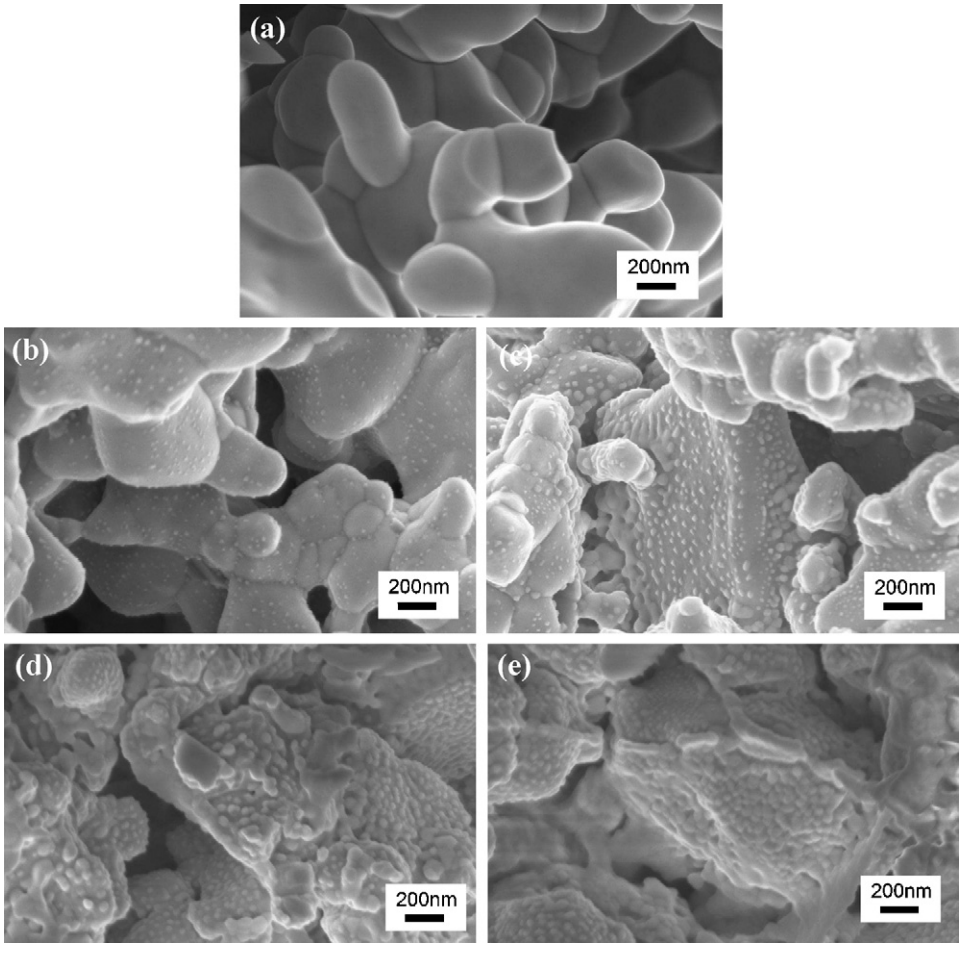

Fig. 2. Cross-sectional views (SEM images) of a blank LSCF cathode (a) and SDC infiltrated LSCF cathodes with different concentrations of SDC solutions: (b) 0.05 mol L^{-1}, (c) 0.10 mol L^{-1}, (d) 0.25 mol L^{-1}, and (e) 0.35 mol L^{-1}.

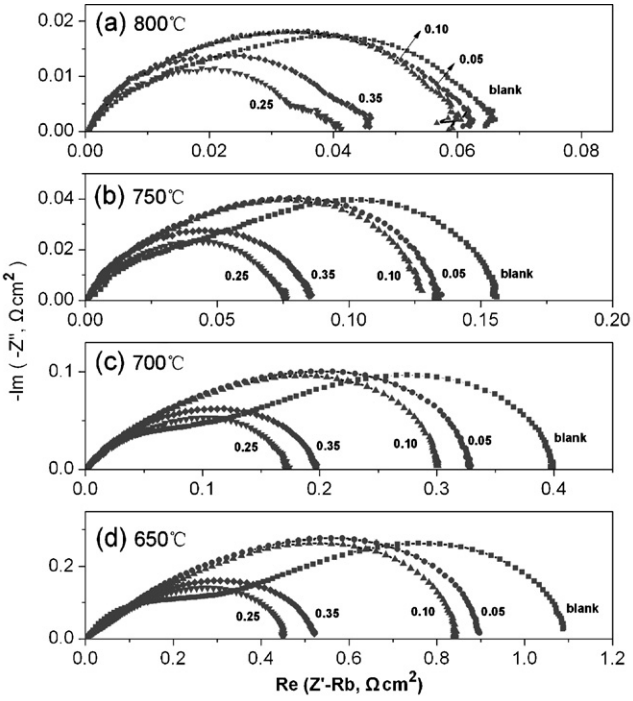

Operating Temperature	ASR of SDC infiltrated LSCF cathode (Ω·cm^2)				
	0	0.05 mol/L	0.10 mol/L	0.25 mol/L	0.35 mol/L
800 °C	0.064	0.061	0.58	0.041	0.045
750 °C	0.15	0.13	0.12	0.074	0.085
700 °C	0.40	0.33	0.30	0.17	0.20
650 °C	1.09	0.89	0.84	0.44	0.52

Fig. 3. Impedance spectra of a LSCF cathode compared with SDC infiltrated LSCF cathodes measured at different temperatures: (a) 800 °C, (b) 750 °C, (c) 700 °C, and (d) 650 °C. The number by each impedance spectrum represents the concentration of SDC solution in mole of SDC per liter (mol L^{-1}).

3. Results and discussion

Fig. 1 shows the XRD patterns of a blank LSCF and an SDC infiltrated LSCF electrode; the primary diffraction lines coincide with those corresponding to the LSCF and SDC phases, and there was no observable evidence for extra phases, demonstrating that the composite has the proper phases.

Shown in Fig. 2 are some typical cross-sectional views of LSCF cathodes infiltrated with different concentrations of SDC. Our previous studies showed that organic solvents, such as ethanol, were an effective additive to improve the wetability on LSCF grains, leading to uniformly distributed coatings on LSCF backbones [13,14]. In this study, a mixture of propanol and water was used to improve the wetting properties of the Sm^{3+} and Ce^{4+} nitrite solution on porous LSCF backbones. Fig. 2a shows a typical view for a porous LSCF cathode prior to infiltration of SDC, indicating that the LSCF backbone was well sintered with the grain sizes in the range of 400–600 nm. After infiltrated with 10 μL 0.05 mol L^{-1} SDC, very fine particles were formed on the LSCF surface with an average particle size of ~20 nm (Fig. 2b). When the concentration of SDC was changed from 0.05 to 0.10 mol L^{-1} (Fig. 2c), uniformly distributed SDC nanoparticles were observed on the surface of LSCF grains with a relatively narrow size distribution and the average particle size was around 40 nm. A higher concentration loading of SDC promoted the nucleation and growth of more and lager nanoparticles, as seen in Fig. 2d. By increasing the concentration of SDC to 0.25 mol L^{-1}, both number and size of nanoparticles continued to increase and a well-connected porous SDC film was formed. The average size of SDC nanoparticles was ~60 nm. When the concentration was increased to 0.35 mol L^{-1}, a continuous film of SDC particles was formed with grain size of ~80 nm. The SDC particles derived from solutions of different concentrations all show a relatively homogeneous distribution on the porous LSCF backbones.

Shown in Fig. 3 are some typical impedance spectra of a blank LSCF cathode and SDC infiltrated LSCF cathodes measured in symmetrical cells under open circuit conditions. In order to clearly show the difference in the electrode polarization behavior, all bulk resistances were removed from the impedance data. The catalytic activity of each electrode, as characterized by the interfacial polarization resistance Rp, was determined from the size of the impedance loop for each electrode. After SDC infiltration, there was a significant reduction in the impedance for O_2 reduction on LSCF electrodes, indicating the enhancement of the electrochemical activity. The area-specific resistance (ASR) of the blank LSCF cathode was 0.064, 0.15, 0.40 and 1.09 Ω cm^2 at 800, 750, 700 and 650 °C, respectively, similar to those reported in the literature [15]. The infiltration of 0.10 mol L^{-1} SDC into the porous LSCF reduced the polarization resistance to 0.12 and 0.84 Ω cm^2 at 750 and 650 °C, respectively. When the concentration of the SDC solution was increased to 0.25 mol L^{-1}, the interfacial resistances were

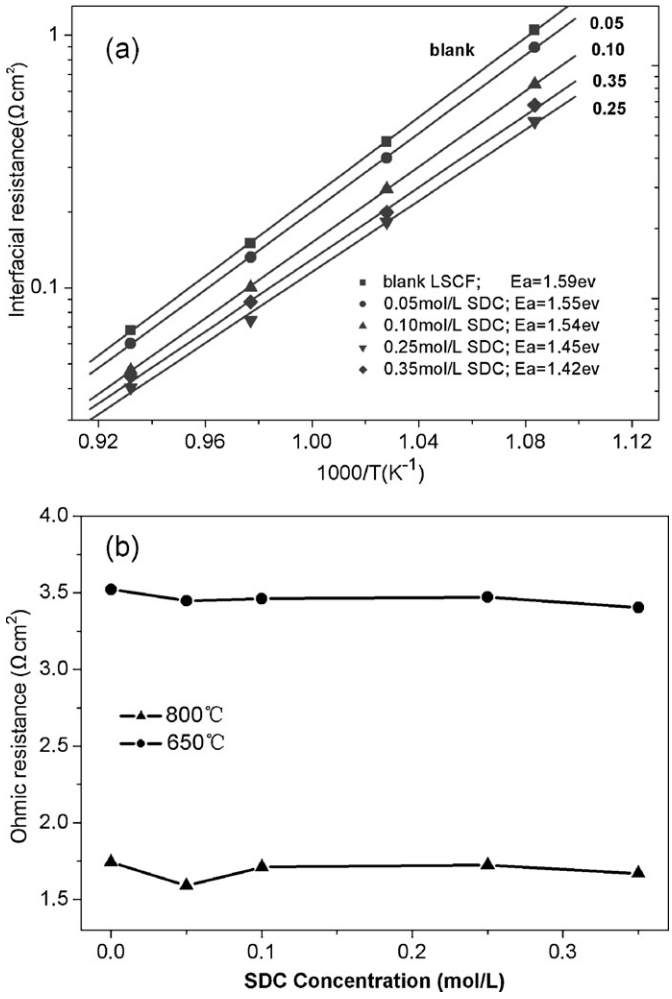

Fig. 4. (a) Activation energies for a blank and SDC infiltrated LSCF cathodes as determined from impedance spectra shown in Fig. 3. The number by each line represents the concentration of SDC solution used for the infiltration in mol L^{-1}. (b) Effect of SDC infiltration on the Ohmic resistances of the test cells.

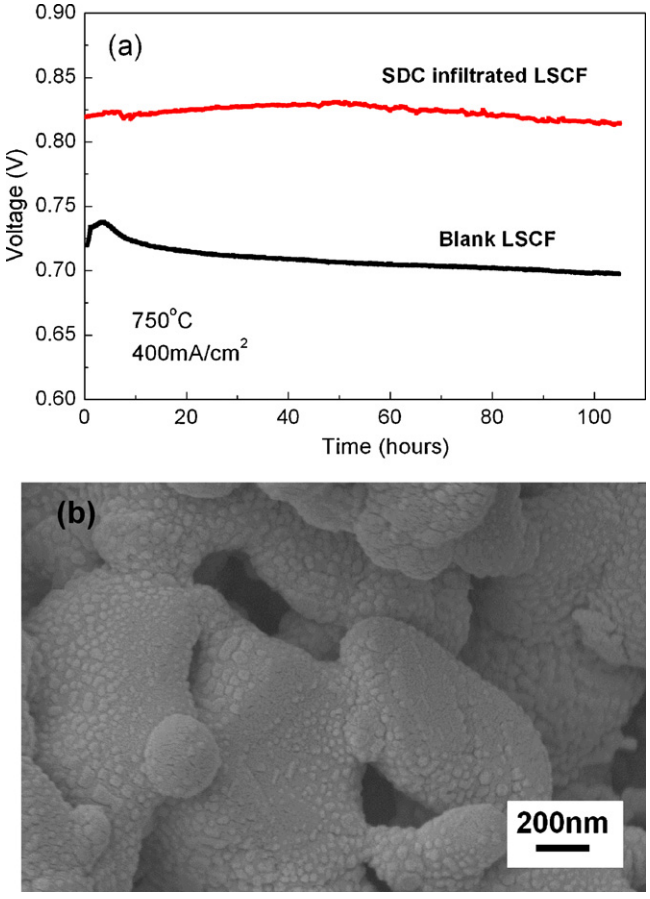

Fig. 5. (a) Performance stability of anode-supported SOFCs with a blank LSCF cathode and an SDC infiltrated LSCF cathode (0.25 mol L^{-1}, 10 μm) operated at a constant current density of 400 mA cm^{-2} at 750 °C for 100 h and (b) a cross-sectional view of the SDC infiltrated LSCF cathode after the stability test at 750 °C for 100 h.

reduced to 0.041, 0.074, 0.17, and 0.44 Ω cm^2 at 800, 750, 700 and 650 °C, respectively, implying more than 50% improvement of the electrochemical performance compared with the blank LSCF cathode. The dramatic decrease in the electrode polarization resistance is mainly attributed to the creation of SDC/LSCF phase boundaries. The newly formed SDC on the LSCF surfaces appears to be highly porous which would allow gas-phase molecules to easily diffuse to the LSCF/SDC boundaries. However, when the concentration of the SDC solution was increased to 0.35 mol L^{-1}, the ASR of the infiltrated cathode became slightly higher than those for the LSCF electrode infiltrated with 0.25 mol L^{-1} SDC. The decrease in electrochemical performance may be explained by the observed microstructure changes, as shown in Fig. 2e. At concentration of 0.35 mol L^{-1}, the SDC coating appeared to be much less porous, reducing the length of the SDC/LSCF phase boundaries so that the electrocatalytic activities of the infiltrated cathode will decrease.

Shown in Fig. 4 are the activation energies for the blank LSCF and the SDC infiltrated LSCF cathodes. The activation energies for the reaction on the SDC infiltrated LSCF cathodes were in the range of 1.42–1.55 eV, slightly lower than the values for the blank LSCF cathode (1.59 eV), but similar to those reported for the LSCF–SDC composite electrodes [9]. The activation energies of SDC infiltrated LSCF are also in agreement with those reported for the LSCF cathode temperature range of 600–800 °C [16,17].

The ohmic resistance of all cells remained almost the same, implying that the infiltration of SDC into LSCF backbone had no observable effect on the bulk resistance of the cells, as clearly shown in Fig. 4b.

Shown in Fig. 5a are the cell voltages of anode-supported SOFCs with blank LSCF and SDC infiltrated LSCF cathode recorded at a constant current density of 400 mA cm^{-2} at 750 °C. During the 100 h of testing, the corresponding cell voltages for the cell with a LSCF cathode ranged from 0.737 to 0.698 V, implying a degradation of more than 5%. As expected from the impedance results above, the cell voltage for the SDC infiltrated LSCF cathode is at a higher value 0.817 V. It is noted that the cell voltage for the cell with SDC infiltrated LSCF cathodes increased to 0.830 V after 50 h but declined to 0.811 V and the degradation rate is ~2%. So SDC infiltration not only reduced the cathodic overpotential but also enhanced cell stability. While a long-term performance degradation of catalysts is usually associated with the coarsening of the microstructure or decomposition of the cathode material [7,18], analysis of the SDC infiltrated LSCF cathodes using SEM (Fig. 5b) showed no observable evidence of particle growth or agglomeration during cell operation.

4. Conclusions

LSCF cathodes coated with nano-sized SDC particles were successfully fabricated by a one-step infiltration method, producing uniformly distributed SDC nanoparticles on the surface of LSCF grains. The SDC infiltrated LSCF cathodes showed significantly

lower electrode polarization resistances than the blank LSCF cathodes at 650–800 °C. The microstructures and performances of SDC infiltrated cathodes depend sensitively on the amount of SDC introduced and the microstructure of the SDC coatings. For the LSCF cathode infiltrated with 10 μL of 0.25 mol L^{-1} SDC, the interfacial resistances were 0.074, and 0.44 Ω cm^2 at 750 and 650 °C, respectively, about half of those for the blank cathode (0.15 and 1.09 Ω cm^2). Furthermore, the infiltrated cell showed improved stability within the time range of testing although the detailed mechanism is yet to be determined. These results indicated that the potential promise of ionic conductor infiltration as a method for enhancing the electrocatalytic activities and stability of MIEC cathodes such as LSCF.

Acknowledgements

This material is based upon work supported by the U.S. Department of Energy SECA Core Technology Program under award number DE-NT0006557 and as part of the Heterogeneous Functional Materials Center, an Energy Frontier Research Center funded by the U.S. Department of Energy, Office of Science, Office of Basic Energy Sciences under Award Number DE-SC0001061.

References

[1] L. Yang, C. Zuo, W. Wang, Adv. Mater. 20 (2008) 3280–3283.
[2] C. Xia, M. Liu, Adv. Mater. 14 (2002) 521–523.
[3] S.P. Jiang, W. Wang, Solid State Ionics 176 (2005) 1351–1357.
[4] M. Liu, D. Dong, R. Peng, J. Power Sources 180 (2008) 215–220.
[5] J. Wang, Z. Lv, X. Huang, J. Power Sources 163 (2007) 957–959.
[6] Y. Liu, S. Zha, M. Liu, Chem. Mater. 16 (2004) 3502–3506.
[7] S.P. Simmer, M.D. Anderson, M.H. Engelhard, Electrochem. Solid-State Lett. 9 (2006) A478–A481.
[8] V. Dusastre, J.A. Kilner, Solid State Ionics 126 (1999) 63–174.
[9] C. Fu, K. Sun, N. Zhang, Electrochim. Acta 52 (2007) 4589–4594.
[10] S.P. Jiang, Y.J. Leng, S.H. Chan, Electrochem. Solid-State Lett. 6 (2003) A67– A70.
[11] M. Shah, S.A. Barnett, Solid State Ionics 179 (2008) 2059–2064.
[12] J. Chen, F.L. Liang, L.N. Liu, S.P. Jiang, J. Power Sources 194 (2009) 275–280.
[13] X. Lou, Z. Liu, S. Wang, J. Power Sources 195 (2010) 419–424.
[14] X. Lou, S. Wang, Z. Liu, Solid State Ionics (2009), doi:10.1016/j.ssi.2009.06.014.
[15] S. Liu, X. Qian, J.Z. Xiao, J. Sol-Gel Sci. Technol. 44 (2007) 187–193.
[16] H. Zhao, L. Huo, L. Sun, Mater. Chem. Phys. 88 (2004) 160–166.
[17] S. Bebelis, N. Kotsionopoulos, A. Mai, J. Appl. Electrochem. 37 (2007) 15–20.
[18] W.S. Wang, M.D. Gross, J.M. Vohs, R.J. Gorte, J. Electrochem. Soc. 154 (5) (2007) B439.